Aggregation dynamics of nonmagnetic particles in a ferrofluid

Jozef Černák*
Department of Biophysics, University of P. J. Šafárik, Jesenná 5, SK-04000 Košice, Slovak Republic

Geir Helgesen and Arne T. Skjeltorp
Institute for Energy Technology, NO-2027 Kjeller, Norway
(Received 1 May 2004; published 29 September 2004)

Nonmagnetic microspheres confined in a ferrofluid layer are denoted by magnetic holes. They form aggregates due to dipolar interactions when an external magnetic field is exerted. Their cluster-cluster aggregation was studied for various magnetic fields using optical microscopy, both for small spheres of diameters, $d=1.9$ and 4 μm, for which Brownian motion was important and for large spheres of diameter, $d=14$ μm, for which Brownian motion was not important. The results for the two smaller sizes were in agreement with standard dynamic scaling theory and the dynamic scaling exponent z for the average cluster length $S(t) \sim t^z$ was found to be slightly smaller than 0.5, while for the largest spheres the z exponent showed a strong dependence on the magnetic-field strength.

DOI: 10.1103/PhysRevE.70.031504 PACS number(s): 83.10.Tv, 75.50.Mm, 82.70.Dd, 89.75.Da

I. INTRODUCTION

Nucleation, aggregation, and formation of complex structures from small subunits like atoms or colloidal particles have been investigated for decades [1]. Studies of structure formation and kinetics during a phase separation are of interest for both theoretical and technological reasons [2]. Although systems with short-range interactions are fairly well understood, our knowledge of processes dominated by long-range interactions is far from complete. In this paper we report experimental studies of the kinetics of magnetic-field induced chains formation of nonmagnetic particles [3] dispersed in thin layers of ferrofluid [4,5].

The kinetics of irreversible aggregation is usually described by Smoluchowski's mean-field theory [6] where coagulation processes can be written in terms of the following reaction scheme:

$$A_i + A_j \xrightarrow{K(i,j)} A_{i+j},$$

where A_i denotes a cluster of mass i. When two clusters of mass i and j meet, they join irreversibly to form a cluster of mass $i+j$ at a rate governed by the constant $K(i,j)$. Smoluchowski's kinetics theory well describes systems characterized by a low concentration of particles with only binary collisions among clusters; spatial correlations of the condensed phase are not considered, i.e., the interactions are of short range.

Meakin [7], and independently Kolb, Botet, and Jullien [8], developed a computer aggregation model of Brownian particles which stick together to form rigid clusters. They generalized the diffusion limited aggregation model (DLA) [9], where only single particles can diffuse, allowing diffusion of all clusters. This model is denoted the cluster-cluster aggregation (CCA) model [2] where the newly formed clusters diffuse along with the single particles and continue to grow by aggregation when they meet other clusters or particles. If the particles are joined together on a first contact it is referred to as the diffusion limited cluster aggregation (DLCA) model [2]. These computer models remove some limitations of the mean-field Smoluchowski theory and enable studies of higher concentrations of particles taking into account the spatial and long-range correlations among them. Vicsek and Family [10] found universal properties of the DLCA mass conservative model for two-dimensional (2D) systems. The cluster size distributions as function of cluster size and time obey a dynamic scaling form.

The DLA [9] and DLCA [7,8] models were developed to describe the formation of fractal objects. Miyazima *et al.* [11] applied ideas from these models also to aggregation of oriented anisotropic rodlike particles that form linear structures. The DLCA model also reflects the main features of aggregation in ferrofluids were all dipolar particles are aligned into chains in the external field direction [12,13].

Experimental studies of colloidal aggregation have been carried out, for example, with paramagnetic microspheres [14,15], nanoparticles [16,17], sulfonated polystyrene latex spheres in colloidal monolayer [18], and electric-field-induced association of dielectric particles [19]. The results have essentially confirmed the scaling behavior of the mean cluster size as a function of time [7,8,11] and it has been possible to scale the temporal size distribution of clusters [14,17,18] into a single universal curve as predicted by dynamic scaling theory [10].

The scaling exponents are constants that classify the growth process. A few experiments have shown that under specific conditions the scaling exponents can deviate from the theoretically predicted or simulated values. The fractal dimension of objects created by growth processes can be influenced by the growth velocity [20], the coupling constant of the dipole-dipole interaction among paramagnetic particles [14], or the relative coverage of the aggregates [21]. Variations in the growth dynamics have also been observed during magnetic-field induced aggregation of paramagnetic

*Electronic address: jcernak@kosice.upjs.sk

microspheres. In particular, the scaling exponent z for the temporal dependences of the mean cluster size $S(t) \sim t^z$ was influenced by the strength of the dipole-dipole interaction with variations $z=1.4-1.7$ [14] and $z=0.45-0.75$ [15], in contrast to the simulated values $z=1.4$ [10] and $z=0.5$ [11] for weak and strong dipolar interactions, respectively. Values of $z=\frac{2}{5}$ for electrorheological fluid aggregation [22] and $z \approx 1.0$ for magnetic latex particle aggregation [23] have also been reported.

In the present work we have studied the chain formation of nonmagnetic microspheres dispersed in a thin layer of ferrofluid [3] induced by external magnetic fields. Experimental data are discussed in the framework of dynamic scaling theory [10], previous experiments on other colloidal systems [14,15], and computer simulations [11,24,25]. In particular, we have tried to investigate the specific conditions that influence the scaling exponent z.

The paper is organized as follows: Secs. II and III contain a description of the basic properties of ferrofluids and magnetic holes that are relevant for our study; Sec. IV contains the experimental setup and method; Sec. V a summary of dynamic scaling theory; Sec. VI the experimental results; and Sec. VII contains the discussion.

II. FERROFLUIDS

A ferrofluid is a suspension of single-domain magnetic particles of a typical diameter $d \approx 10$ nm dispersed in a carried fluid [4,5]. The particles mostly used are made from magnetite, Fe_3O_4, but other materials are also employed [26]. If two colloidal particles come close together, the van der Waals forces will irreversibly bind them together. This has to be prevented in order to make stable ferrofluids. This attractive interaction can be overcome by introducing additional repulsive interactions (steric or Coulombic) between the particles. The steric repulsion is realized by a surfactant on the particles. If the carrier fluid is water, the Coulombic stabilization takes place via a volume charge created around the nanoparticles with appropriate ions.

Ferrofluids have rich physical behaviors with unconventional rheological, thermal, magnetic, optical, and electrical properties with many applications [4,5]. In fact, the uses of ferrofluids were early examples of nanotechnology. One of the simplest physical model of ferrofluids is based on the assumptions that magnetic particles are spherical without electrostatic charge and that the van der Waals interaction between two such spheres is negligible. When external magnetic fields are applied, then long-range dipole-dipole interaction between arbitrary two grains dominate and the particles tend to form chains aligned with the magnetic field **H** [27]. Earlier experimental works confirm the existence of chains or needles [12,21] and support the picture predicted by de Gennes and Pincus [27] in the zero magnetic-field limit where randomly oriented chains of various sizes and form and closed rings are formed [28], similar to a polydisperse polymer melt. Recent results obtained by cryogenic transmission electron microscopy [29] demonstrate the existence of dipolar chain structures in a ferrofluid without an external magnetic field.

III. MAGNETIC HOLES

Magnetic holes are nonmagnetic voids in a ferrofluid. By using monodisperse polystyrene microspheres prepared by the Ugelstad method [30] very uniformly sized magnetic holes may be created. The microspheres are much larger ($1-100$ μm) than the magnetic particles in the ferrofluid (typically 0.01 μmm) so they move in an approximately uniform background. When an external magnetic field **H** is applied, the void produced by a single microsphere possesses an effective magnetic moment equal in size but opposite in direction to the magnetic moment of the displaced fluid:

$$\mathbf{m}_i = -\chi_{\text{eff}} V \mathbf{H}, \tag{1}$$

where χ_{eff} is the effective volume susceptibility and V is the volume of the sphere [3]. Including the demagnetization factor, $\chi_{\text{eff}} = \chi/(1+2\chi/3)$ for a spherical magnetic hole, where χ is the susceptibility of the ferrofluid. Two magnetic holes with magnetic moments $\mathbf{m}_i$ and $\mathbf{m}_j$ interact via an anisotropic dipolar potential,

$$U_{ij}^{dip} = \frac{\mu_0}{4\pi} \frac{\mathbf{m}_i \cdot \mathbf{m}_j - 3(\hat{\mathbf{r}} \cdot \mathbf{m}_i)(\hat{\mathbf{r}} \cdot \mathbf{m}_j)}{r^3}, \tag{2}$$

where $\mathbf{r}$ is the vector between particle centers and $\hat{\mathbf{r}}$ is the unit vector $\mathbf{r}/r$. The dimensionless interaction strength parameter λ, which characterizes the strength of the dipole-dipole interaction relative to the disruptive thermal energy, is defined as

$$\lambda = \frac{U_{\max}^{dip}}{kT}, \tag{3}$$

where k is Boltzmann's constant and T is the temperature.

The main advantage of this systems is the possibility to model a broad range of physical phenomena from aggregation to the complex dynamic of many-body systems [31]. In our case we can create experimental conditions that are close to the theoretical assumptions of Ref. [27], i.e., the particles are spherical, monodisperse, and their resulting induced magnetic moments are oriented in the direction of the external magnetic field. In order to study the importance of dipole-dipole interaction and Brownian motion relative to non-Brownian ballistic drift, we used microspheres with different diameters $d=1.9$, 4, and 14 μm. In zero external magnetic fields the diffusive Brownian motion of the 1.9-μm spheres is clearly visible in the microscope. However, the diffusion of the 14-μm spheres can only be seen by comparing images taken at typically 30-sec. time intervals.

IV. EXPERIMENT

The experimental setup shown in Fig. 1 consists of an optical microscope (Nikon Optiphot) with a video adapter, one pair of coils, and a carefully prepared sample. A video camera (JVC charge-coupled device with resolution 768×576 pixels), a digital camera (Nikon Coolpix with resolution 1600×1200 pixels) and a personal computer were used to capture, store, and analyze the microscopic images.

The sample of size about 20×20 mm consisted of polystyrene microspheres dispersed in a thin layer of ferrofluid

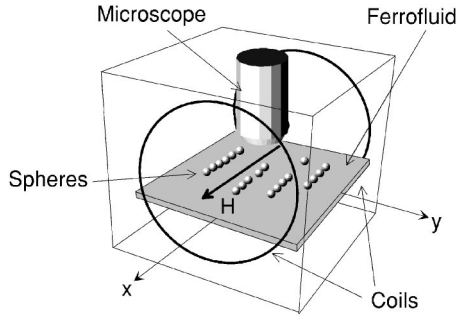

FIG. 1. The experimental setup used to study aggregation of polystyrene microspheres.

which was confined between two glass plates and sealed. A very low concentration of larger microspheres of diameter $d=50$ μm was used as spacer to keep an even layer thickness of the kerosene based ferrofluid [32] which was used. The physical properties were: density $\varrho=1020$ kgm^{-3}, susceptibility $\chi=0.8$, saturation magnetization $M_s=20$ mT, and viscosity $\eta=6\times10^{-3}$ Nsm^{-2}.

The experiments were performed at room temperature, using magnetic-field intensities in the range $H=100-1300$ A m^{-1}, and a relative volume fraction (or coverage) of particles $\phi=0.002-0.10$. Starting from a random initial configuration of polystyrene microspheres inside the ferrofluid layer, a constant magnetic field **H** parallel to the layer was switched on. The field-induced aggregation was captured at definite time intervals. The total duration of an observation was up to 3 h. The number of clusters and their size (length) were determined by analyzing the optical micrographs. Two independent image processing methods were used to analyze the microscopic pictures and they gave approximately the same results.

V. DYNAMIC SCALING THEORY

Here we summarize some of the notations and relevant findings of dynamic scaling theory that will be used later. The number of clusters with the same size s is denoted $n_s(t)$, representing the cluster size distribution at time t. $N(t)=\Sigma_s n_s(t)$ is the total number of clusters. The weighted mean cluster size is given by [10]

$$S(t)=\frac{\sum_s n_s(t)s^2}{\sum_s n_s(t)s}. \tag{4}$$

The temporal evolution of a cluster-cluster aggregation processes is characterized by a power-law time dependence of the mean cluster size

$$S(t)\sim t^z, \tag{5}$$

and the cluster size distribution $n_s(t)$ at time t. Dynamic scaling theory [10] predicts the following scaling relationship between these quantities:

$$n_s(t)\sim t^{-w}s^{-\tau}f(s/t^z) \tag{6}$$

or in an alternative form:

$$n_s(t)\sim s^{-2}g(s/t^z). \tag{7}$$

Here $f(x)$ is a cutoff function with $f(x)\simeq1$ for $x\ll1$ and $f(x)\ll1$ for $x\gg1$. $g(x)$ is a scaling function, $g(x)\ll1$ for $x\gg1$ and $g(x)\sim x^{\Delta}$ for $x\ll1$, where Δ is called the crossover exponent. Based on the assumption that the aggregation is mass independent, the following relationships between these scaling exponents were derived [10]:

$$w=z\Delta \tag{8}$$

and $\tau=2-\Delta$.

Using expression Eq. (6) it was found [2,33] that

$$N(t)\sim t^{-z'}\equiv\begin{cases}t^{-z} & \text{for } \tau<1\\ t^{-w} & \text{for } \tau>1.\end{cases} \tag{9}$$

The dynamic scaling theory [10] was generalized by Meakin *et al.* [33] in the case when the diffusion coefficient D_s for a cluster of mass s was given by

$$D_s=D_0s^{\gamma}, \tag{10}$$

where D_0 is a constant and γ is the diffusion exponent ($\gamma=0$ means mass independent diffusion). The theoretical prediction for the crossover exponent Δ is

$$\Delta=\begin{cases}(2-\tau) & \text{for } \gamma>\gamma_c\\ 2 & \text{for } \gamma<\gamma_c,\end{cases} \tag{11}$$

where γ_c is a critical value of γ at which aggregation dynamics changes from being dominated only by the large cluster–small cluster interactions (below γ_c) to a dynamics where large-small and large-large clusters processes are equally important. Also, the shape of the cluster-size distribution n_s crosses over from a monotonically decreasing function of cluster size s above γ_c to a bell-shaped curve below. It was believed that in 2D $\gamma_c\simeq-\frac{1}{4}$ and in 3D $\gamma_c\simeq-\frac{1}{2}$ [33,34], but more recent simulations have shown that $\gamma_c\approx0$ in one dimension while the shape of the cluster size distribution changes at $\gamma\sim0.7$ [35]. It was then argued by Hellén *et al.* [35] that $\gamma_c=0$ in higher dimensions too.

VI. RESULTS

One typical result of the aggregation process is shown in the micrographs in Fig. 2 with the growth of clusters of 4-μm magnetic holes. Figure 2(a) shows the initial state without a magnetic field ($H=0$). As may be seen, the spheres are at random positions within the ferrofluid layer. The nonmagnetic spheres can move randomly as they are subject to Brownian motion. As soon as a constant external magnetic field H is applied parallel with the sample surface, the field-induced aggregation starts as seen in Figs. 2(b) and 2(c) and with a gradual increased chaining of the particles with time along the field direction as a result of their field-induced magnetic moment m_i. It was observed that when two particles were close they stuck and remained joined together on first contact in an irreversible aggregation process. All the clusters formed were straight and looked similar to those found in electric field induced colloidal aggregation [19]. However, for $\lambda\leqslant1$ fractal aggregates can form [14,36]. For

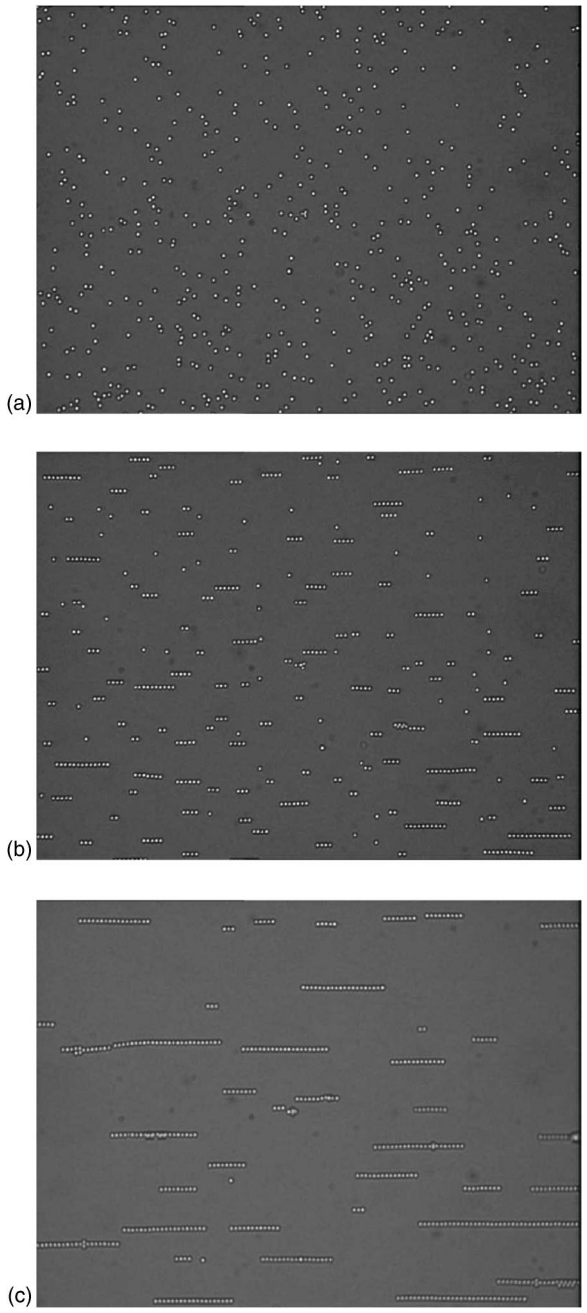

FIG. 2. Optical micrographs of the aggregation of $d=4$-μm microspheres at different times: (a) $t=0$ s, (b) $t=417$ s, and (c) $t=5019$ s after a magnetic field $H=800$ A m^{-1} was turned on.

high particle volume fractions, $\phi>0.2$, we saw some degree of sidewise coalescence of chains [13].

In order to characterize the aggregation process in more detail, the length s of any cluster was determined at different time intervals t relative to the initial time $t=0$ when the field was turned on. The time dependences of the number of clusters $N(t)$ and mean cluster size (length) $S(t)$ for a typical experiment with $d=4$-μm particles are shown in Fig. 3. We see that the data asymptotically follow the power laws $N(t) \sim t^{-z'}$ and $S(t) \sim t^{z}$ with scaling exponents $z'=0.43\pm0.01$ and $z=0.40\pm0.01$ for $t>60$ s.

Figure 4 shows the scaling functions $g(x)$ as presented in

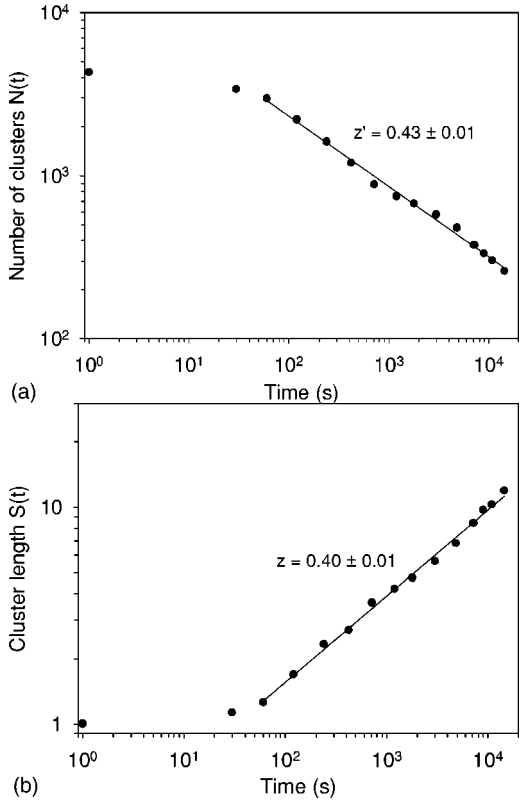

FIG. 3. (a) The number of clusters $N(t)$ and (b) the mean (weight average) cluster length $S(t)$ [Eq. (4), in units of sphere diameters] versus time for an experiment with $d=4$-μm microspheres at $\lambda=370$. The best fits for the corresponding scaling exponents z' and z are shown as solid lines.

Eq. (7) for the data in Fig. 3. As may be seen, the data obtained at times $t<100$ s deviate from a common curve for $s/S(t)\leqslant 1$. On the other hand, for time $t>100$ s where the average cluster size $S(t)$ obeys a power law, the data scale

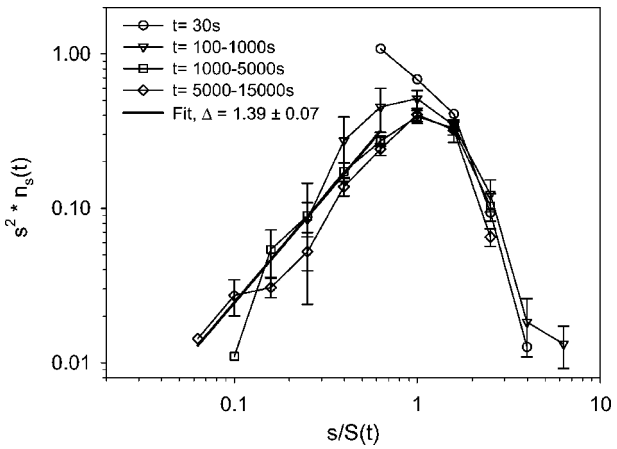

FIG. 4. The scaling function $g(x)=s^2 n_s(t)$ obtained from the cluster size distributions $n_s(t)$ at interaction strength $\lambda=370$. The cluster size distributions plotted are for the single time instant $t=30$ s and average values for the time intervals $t=100-1000$ s, 1000–5000 s, and 5000–15 000 s. For $x<1$ and time $t>100$ s the data have been fitted to a power law $g(x)\sim x^{\Delta}$ with exponent $\Delta=1.39\pm0.07$.

properly with a crossover exponent $\Delta = 1.39 \pm 0.07$ for $s/S(t) < 1$ and times in the range $t = 100 - 15\,000$ s.

Microspheres with diameters $d = 1.9$, 4, and 14 μm and magnetic-field intensity H in the range $200 < H < 1300$ A m^{-1} were used to get values of the interaction strength parameter λ [Eq. (3)] in the range $8 < \lambda < 1.6 \times 10^4$. The relative volume fraction of microspheres was relatively low, typically $\phi = 0.02 - 0.04$. The results show a small dependence of the scaling exponent z on the parameter λ and on particle diameter. For the smallest particle diameter $d = 1.9$ μm, the scaling exponent z is independent of λ in the parameter range $\lambda = 8 - 50$. The average value of the scaling exponent is $z = 0.42 \pm 0.06$ which is somewhat lower than the predicted value $z = 0.5$ [11,25]. For larger particles with diameter $d = 4$ μm, we have observed a somewhat broader range of z values, $z = 0.45 \pm 0.10$, as compared to those for the smallest particles. A fit to a linear relationship between z and λ for $\lambda = 8 - 500$ gives $z(\lambda) = 0.409 + 2.053 \times 10^{-4}\lambda$.

Quite different results were obtained for the biggest particles with diameter $d = 14$ μm. For these particles there were a very strong dependence of z on the λ parameter. The value of z reached very low values, $z < 0.25$, for $\lambda < 3000$. For parameter λ in the interval $10^3 < \lambda < 10^4$, the scaling exponent $z(\lambda)$ grows almost linearly with $\log(\lambda)$ up to a maximum value $z \approx 0.6$ and could be fitted as $z(\lambda) \approx -1.33 + 0.47 \times \log_{10}(\lambda)$. The cluster size distributions $n_s(t)$ for the 14-μm particles could also be scaled into a scaling function as shown in Fig. 7 for $\lambda = 3470$. The best fit for the exponent Δ, $\Delta = 1.83 \pm 0.09$, is shown as a solid line in this figure. Generally, the data collapse to a scaling function $g(x)$ was worse for the 14-μm particles than for the smaller sizes.

The fitting results for the exponents z, z', and Δ for all particle sizes and some selected experiments are summarized in Table I, along with a few of the exponent values reported earlier in the literature for low values of λ. As seen, our results for the values of z and z' are often nearly equal. For these cases the value of Δ is close to $\Delta = 1.5$. Otherwise, the value of Δ is considerably higher.

TABLE I. The characteristic exponents of the dynamics scaling theory z, z', and Δ for different particle diameters d, dimensionless magnetic interaction parameter λ, and the volume fraction of particles ϕ.

d (μm)	λ	ϕ	$z(\pm 0.01)$	$z'(\pm 0.01)$	Δ
0.0114[a]	4.6	0.021	0.786	$0.67_{\pm 0.15}$	0.8
0.6[b]	8.6	0.0004	$0.75_{\pm 0.01}$		
0.6[b]	8.6	0.0020	$0.51_{\pm 0.01}$		
0.8[c]	13	0.03	$1.08_{\pm 0.12}$		
1.27[d]	31	0.009	$0.60_{\pm 0.02}$		
3.6[e]	1360		$1.7_{\pm 0.2}$		
1.9	8.0	0.0023	0.42	0.42	$1.42_{\pm 0.12}$
1.9	16.6		0.48	0.46	$1.47_{\pm 0.26}$
1.9	37.0		0.39	0.40	$1.40_{\pm 0.11}$
4	9.1	0.021	0.41	0.38	$1.61_{\pm 0.07}$
4	150	0.0047	0.38	0.44	$1.94_{\pm 0.07}$
4	250		0.48	0.54	$1.88_{\pm 0.10}$
4	340		0.54	0.54	$1.53_{\pm 0.13}$
4	370	0.060	0.40	0.43	$1.39_{\pm 0.07}$
14	1040	0.050	0.084	0.15	$3.20_{\pm 0.19}$
14	2070		0.20	0.26	$2.44_{\pm 0.10}$
14	3470		0.25	0.30	$1.83_{\pm 0.09}$
14	6260	0.036	0.40	0.37	$1.57_{\pm 0.10}$
14	10600	0.037	0.59	0.60	$1.47_{\pm 0.20}$

[a]In Refs. [16,17].
[b]In Ref. [15].
[c]In Ref. [23].
[d]In Ref. [19] (aggregation in electric field).
[e]In Ref. [14].

VII. DISCUSSION

The aggregates formed in our experiments have a rodlike form and may therefore be compared to earlier computer simulations on the aggregation of oriented anisotropic particles [11]. These simulations were based on the following assumptions: (i) the diffusion coefficient D_s for a cluster of mass s was given by Eq. (10); (ii) the direction of motion for a cluster was selected randomly to model a Brownian cluster; and (iii) a strong nearest-neighbor interaction. The scaling behavior of the mean cluster size $S(t)$ given by Eq. (4), $S(t) \sim t^z$, and the number of clusters $N(t) \sim t^{-z'}$, was found in these computer simulations for various values of the diffusion coefficient γ in 2D and 3D systems. The scaling exponents were approximately equal, $z = z'$, in most simulations. In particular, for $\gamma = -1$ in 2D and for low particle concentrations, $z = 0.5$ was found to be a universal value. For highly concentrated samples a crossover to 1D aggregation took place and the scaling exponent z was lower, $z = 1/3$. The cluster size distribution $n_s(t)$ collapsed to a single curve [Eq. (7)] as predicted by the dynamic scaling theory [10]. In contrast to the above assumptions, in our experiments the interactions are of long range and dipolar in character, hydrodynamic couplings may be important, and the diffusion constant may possibly be anisotropic.

Our experimental data show that the total number of clusters $N(t)$ and the mean cluster size $S(t)$ scales with time, see Fig. 3, up to times where the finite size of the observed system becomes important. The scaling exponents z and z' are approximately equal, but slightly lower than the value $z = 0.5$ predicted for a system with $\gamma = -1$ [11]. The cluster size distributions at different times can be scaled into a single curve $g(x)$, see Fig. 4, that supports dynamic scaling theory [10]. For low values of λ these results are in a good qualitative agreement with the scaling found in the DLCA model simulations by Miyazima *et al.* [11], but with minor quantitative deviations.

A detailed study of the influence of the interaction strength parameter λ and particle diameter d on the scaling exponent z, shows a more complex $z(\lambda)$ dependence as seen in Fig. 5. For the smallest particles $d = 1.9$ μm and $\lambda = 8 - 50$, the average scaling exponent $z = 0.42 \pm 0.06$ is independent on the parameter λ and is significantly lower than

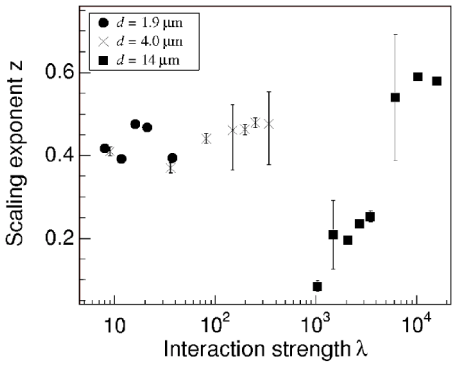

FIG. 5. The scaling exponents z as a function of the dimensionless parameter λ [Eq. (3)] for microspheres of diameter: $d=1.9$, 4, and 14 μm.

the value $z=0.5$ found in computer simulations [11], in experimental works on dipolar magnetic nanoparticles [17] ($z=0.786$), and for superparamagnetic latex particles [15] ($z=0.45-0.75$). However, it is close to the value $z=0.40$ found for aggregation in an electrorheological fluid [22]. The finding of an apparently weak increase in the value of z for $\lambda>50$ is opposite to what was reported by Promislow *et al.* [15] who found a decrease in z for larger λ.

For the largest particle size ($\lambda \geqslant 10^3$) the z exponent is strongly dependent on magnetic-field strength, or λ, and there was almost no growth for the weakest fields. The field dependence is probably due to a more dominating effect of the field-induced, ballistic motions of the microspheres. Low growth rate can also possibly be due to direct contact, or even sticking, between the microspheres and one of the glass plates when the Brownian motion is small and the self-centering repulsion force [3,37,38] from the boundary conditions is weak. For parameter $\lambda>5000$ the value of the scaling exponents z is in the range found for the smaller particles sizes and in other experiments on DLCA [15]. $z(\lambda)$ increases up to about $z\approx 0.6$. This is clearly larger than the theoretically expected $z=0.5$, but agrees with previous results [15]. Increasing values of the scaling exponent $z(\lambda)=0.5\rightarrow 0.8$ have been found in computer simulations of ferromagnetic colloidal particles [24] for $7<\lambda<13$. A value of $\lambda\sim 800$ at the transition between diffusion dominated and field (ballistic drift) dominated aggregation may seem high. However, the typical interaction energy involved is much less since this is the interaction energy at typical interparticle distances. This typical distance is $\sim 1/\sqrt{\phi}\approx 5$ particle diameters for a relative volume fraction $\phi=0.04$. Since $U\sim r^{-3}$, then a typical magnetic energy is $U\sim(\lambda/125)$ kT≈ 5 kT and of the order of magnitude as one would expect.

Miguel *et al.* [25] have taken into account hydrodynamic interactions in computer simulations of a dipolar, anisotropic DLCA model. Their basic assumption was that the diffusion coefficients were different for parallel, $D_{\parallel}$, and perpendicular, $D_{\perp}$, orientation relative to the rod's axis and were given by

$$D_{\parallel}\sim\frac{\ln s}{s},\ D_{\perp}\sim\frac{D_{\parallel}}{2}. \tag{12}$$

The logarithmic correction of the diffusion coefficients $D_{\parallel}$ and $D_{\perp}$ incorporated the dependence on the shape of the clusters and lead to a functional dependence of the average cluster size of the form

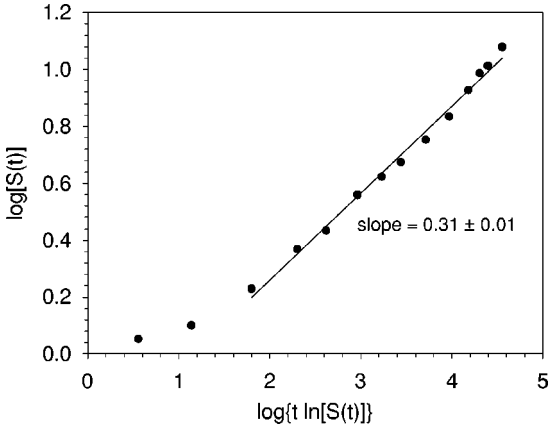

FIG. 6. The weighted average chain length $S(t)$ (in units of sphere diameters) with the effects of anisotropic diffusion taken into account. The experimental data are the same as in Fig. 3(b).

$$S(t)\sim\{t\ln[S(t)]\}^{\zeta}, \tag{13}$$

where $\zeta=d/(2+d)$ for $d\leqslant d_c=2$ and $\zeta=\frac{1}{2}$ otherwise.

In order to be able to compare to the predictions of the anisotropic diffusion model of Miguel *et al.* [25], we have in Fig. 6 replotted the cluster length data shown in Fig. 3(b) using the functional form of Eq. (13). The exponent of the power-law dependence $\zeta=0.31\pm0.01$ was clearly lower than the value $z=0.40\pm0.01$ found using the normal isotropic scaling assumptions. The goodness of fit was not improved using the new functional form. Similar changes were obtained when other datasets were replotted according to Eq. (13). In Ref. [25] it was reported that computer simulations on an anisotropic diffusion model in two dimensions gave $z=0.61$ assuming the standard scaling form in Eq. (5) and $\zeta=0.51$ using the anisotropic scaling form in Eq. (13). Our values of z and ζ are clearly lower. For $\lambda\geqslant 10^4$, $z\approx 0.6$ and we find $\langle\zeta\rangle=0.53\pm0.02$ which is in agreement with the findings of Miguel *et al.* [25] for their dipolar, anisotropic DLCA model.

In most of the experiments the cluster size distributions $n_s(t)$ were found to scale into a scaling function $g(x)$ as given by Eq. (7). The asymptotic behavior of the scaling functions $g(x)$ can be expressed as $g(x)\sim x^{\Delta}$ or $g(x)\sim\exp(-x^{-|\mu|})$ as $x=s/S(t)\rightarrow 0$, depending on the details of how clusters join [34,35]. Two examples are shown in Figs. 4 and 7 for $\lambda=370$ and 3470, respectively. For the case shown in Fig. 4 the scaling exponents were nearly equal, $z=0.40$ and $z'=0.43$, and the best-fit value for the crossover exponent was $\Delta=1.39\pm0.07$. Figure 7 shows a borderline case where the value of z is just below the lower limit for validity of the DLCA description, $z\geqslant\frac{1}{3}$. Here $z=0.25$ and $z'=0.30$, and the crossover exponent Δ was found to be $\Delta=1.83$. However, the scaling function still seems to have a power-law behavior for small $x=s/S(t)$. In a few experiments with low values of z, or at early times in some other experiments, the decay at small x was faster than a power law. In Table I we compare

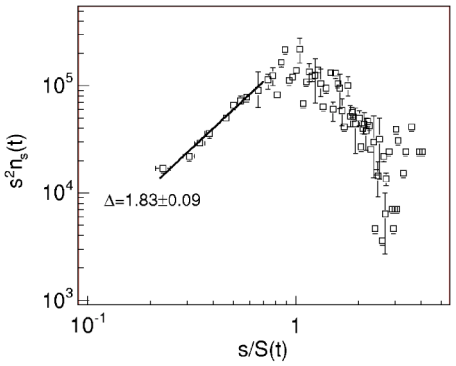

FIG. 7. The scaling function $g(x)=s^2n_s(t)$ obtained from the size distributions $n_s(t)$ for $d=14$-μm particles with interaction strength $\lambda=3470$. For $x<1$, $g(x)\sim x^{\Delta}$ with $\Delta=1.83\pm0.09$ was found. The scaling exponents for this experiment were: $z=0.25$, $z'=0.30$, and the maximum observation time was $t_{max}=6120$ s.

some of our measured values for the scaling exponents to earlier reported experimental values. The values of z are clearly lower than what have been reported before in the literature.

Since we found that $\Delta>1$ in all cases, the value of τ, $\tau=2-\Delta<1$, and then from Eq. (9) $z'=z$. This is nearly fulfilled within the experimental uncertainty for those cases in Table I where the value of Δ is clearly smaller than 2. For those with $\Delta>1.8$, the values of z and z' are different and the assumptions of the DLCA model may not be fulfilled. For two of the cases $\Delta>2$ and z, $z'<\frac{1}{3}$ which is the z value for 1D systems [11,25], and we are outside the applicability of the DLCA model. Observation of a scaling function behavior $g(x)\sim x^{\Delta}$ is similar to the earlier reported measurements of nanoparticle aggregation [17] ($d=0.0114$ μm in Table I). In that case $\tau=2-\Delta>1$, $z'=w$ and the exponents satisfy the exponent relation in Eq. (8). In the present case with $\tau<1$, we cannot get the exponent w directly from the data.

For several model systems it has been found that $z=1/(1-\gamma)$ where γ is the diffusion exponent of Eq. (10). For the values of z, $0.4<z<0.5$, found for the two smallest particle sizes this relation will give γ values in the range $-1.5<\gamma<-1.0$, which is smaller than the critical value $\gamma_c(2D)\simeq-\frac{1}{4}$ [33]. For this case $\tau<1$ and Eq. (9) shows that $z'=z$, which was fulfilled in many of our measurements. With $\gamma<\gamma_c$, then $\Delta=2$ according to Eq. (11), which was not the case here, and one should not have seen the power-law behavior found in our data. Our measurements fit better to the case $\gamma>\gamma_c$, with $\tau=2-\Delta\approx0.5$, which is also consistent with $z'=z$ from Eq. (11). However, it may be pointed out that for $s/S(t)\ll1$ the statistics in our data is limited and our estimates of Δ are lower limits, so it cannot be excluded that $\Delta\to2$ in the asymptotic limit.

The results from the largest ($d=14$ μm) particles with a very strong dependence of z on λ are, to our knowledge, not consistent with any of the cluster aggregation models proposed so far. For large particles with small Brownian motions and long-range interactions, one might expect that the ballistic dynamics is dominating. In simulations of 1D field-driven cluster-cluster aggregation (FDCA) by Hellén *et al.* [35] it was found that the value of z depended on the value of the velocity of the ballistic motions and the value was found to vary from 0.4 to well above 2. In that work it was assumed that the ballistic velocity of the clusters varied as $v\sim s^{\delta}$. In our case, the interaction between clusters is proportional to the cluster volume, i.e., the size, and $\delta\approx1$. For 1D systems $\delta=1$ is the value for crossover to gelling. Below this value and the line $\delta=\gamma-1$ in the (γ,δ) phase diagram, the 1D scaling function $g(x)$ should depend exponentially on x and not show power-law behavior as we apparently see in two dimensions.

Preliminary results from computer simulations on a detailed model for field-induced aggregation of large magnetic holes in a 2D layer [39] show a behavior with $z=0.50$ in agreement with earlier simulation results [11]. However, the exploration of the full 2D and 3D (γ,δ), or diffusion versus field, phase diagram is still a challenge.

VIII. CONCLUSIONS

The field-induced aggregation of nonmagnetic microspheres inside a ferrofluid layer has been studied. The scaling behaviors of the average chain length $S(t)$ and number of clusters $N(t)$ where found for a range of values of the dimensionless interaction strength λ. The chain length distributions $n_s(t)$ could be transformed into a scaling function $g(x)$ as required in DLCA, but the exponents z and Δ of the dynamic scaling theory were found to depend on the interaction strength λ.

For microspheres with diameters $d=1.9$ and 4 μm, the exponent z of the cluster length, $S(t)\sim t^z$, was found to be $z\approx0.42$ in a broad interval of the λ parameter: $8<\lambda<500$. There was a slight increase in z with larger λ. In the case of the largest microspheres, $d=14$ μm, the scaling exponent z was strongly dependent on λ for $\lambda>1000$ with values in the interval $0.08<z\leqslant0.6$. However, scaling exponents $z<\frac{1}{3}$ are inconsistent with the DLCA model.

The cluster number exponent z', $N(t)\sim t^{z'}$, was found to be nearly equal to z, and clearly different from the exponent $w=z\Delta$. The relations among the scaling exponents found for DLCA models with short-range interactions were not fulfilled in this system. This may be due to the long-range nature of the dipole-dipole interactions in the system and the partly ballistic character of the particle motions.

ACKNOWLEDGMENTS

The main part of this work was done at the Institute for Energy Technology (IFE, Kjeller). J.C. thanks for kind hospitality the Department of Physics at IFE. We acknowledge financial support from the Slovak Ministery of Education: Grant Nos. Nor/Slov and Nor/Slov2002.

[1] V. J. Anderson and H. N. W. Lekkerkerker, Nature (London) **416**, 811 (2002).
[2] T. Vicsek, *Fractal Growth Phenomena*, 2nd ed. (World Scientific, Singapore, 1992).
[3] A. T. Skjeltorp, Phys. Rev. Lett. **51**, 2306 (1983).
[4] R. E. Rosensweig, *Ferrohydrodynamics* (Cambridge University Press, Cambridge, England, 1985).
[5] B. M. Berkovsky, V. F. Medvedev, and M. S. Krakov, *Magnetic Fluids—Engineering Aplications* (Cambridge Univesity Press, Oxford, 1993).
[6] M. von Smoluchowski, Phys. Z. **17**, 585 (1916).
[7] P. Meakin, Phys. Rev. Lett. **51**, 1119 (1983).
[8] M. Kolb, R. Botet, and R. Jullien, Phys. Rev. Lett. **51**, 1123 (1983).
[9] T. A. Witten, Jr. and L. M. Sander, Phys. Rev. Lett. **47**, 1400 (1981).
[10] T. Vicsek and F. Family, Phys. Rev. Lett. **52**, 1669 (1984).
[11] S. Miyazima, P. Meakin, and F. Family, Phys. Rev. A **36**, 1421 (1987).
[12] C. F. Hayes, J. Colloid Interface Sci. **52**, 239 (1975).
[13] A. Satoh, R. W. Chantrell, S.-I. Kamiyama, and G. N. Coverdale, J. Colloid Interface Sci. **178**, 620 (1996).
[14] G. Helgesen, A. T. Skjeltorp, P. M. Mors, R. Botet, and R. Jullien, Phys. Rev. Lett. **61**, 1736 (1988).
[15] J. H. E. Promislow, A. P. Gast, and M. Fermigier, J. Chem. Phys. **102**, 5492 (1995).
[16] J. Černák, P. Macko, and M. Kašparková, J. Phys. D **24**, 1609 (1991).
[17] J. Černák, J. Magn. Magn. Mater. **132**, 258 (1994).
[18] D. J. Robinson and J. C. Earnshaw, Phys. Rev. A **46**, 2045 (1992); **46**, 2055 (1992); **46**, 2065 (1992).
[19] S. Fraden, A. J. Hurd, and R. B. Meyer, Phys. Rev. Lett. **63**, 2373 (1989).
[20] A. T. Skjeltorp, Phys. Rev. Lett. **58**, 1444 (1987).
[21] H. E. Horng, C.-Y. Hong, S. Y. Yang, and H. C. Yang, J. Phys. Chem. Solids **62**, 1749 (2001).
[22] J. E. Martin, J. Odinek, and T. C. Halsey, Phys. Rev. Lett. **69**, 1524 (1992).
[23] D. Sohn, J. Magn. Magn. Mater. **173**, 305 (1997).
[24] H. Morimoto and T. Maekawa, J. Phys. A **33**, 247 (2000).
[25] M. C. Miguel and R. Pastor-Satorras, Phys. Rev. E **59**, 826 (1999).
[26] F. A. Tourinho, R. Franck, and R. Massart, J. Mater. Sci. **25**, 3249 (1990).
[27] P. G. de Gennes and P. A. Pincus, Phys. Kondens. Mater. **11**, 189 (1970).
[28] W. J. Wen, F. Kun, K. F. Pál, D. W. Zheng, and K. N. Tu, Phys. Rev. E **59**, R4758 (1999).
[29] K. Butter *et al.*, Nat. Mater. **2**, 88 (2003).
[30] J. Ugelstad and P. C. Mork, Adv. Colloid Interface Sci. **13**, 101 (1980).
[31] G. Helgesen and A. T. Skjeltorp, J. Appl. Phys. **69**, 8277 (1991).
[32] Type EMG 909, produced by FerroTec, Nashua, New Hampshire.
[33] P. Meakin, T. Vicsek, and F. Family, Phys. Rev. B **31**, 564 (1985).
[34] P. G. J. van Dongen and M. H. Ernst, Phys. Rev. Lett. **54**, 1396 (1985).
[35] E. K. O. Hellén, T. P. Simula, and M. J. Alava, Phys. Rev. E **62**, 4752 (2000).
[36] Z. J. Tan, X. W. Zou, W. B. Zhang, and Z. Z. Jin, Phys. Rev. E **62**, 734 (2000).
[37] M. Warner and R. M. Hornreich, J. Phys. A **18**, 2325 (1985).
[38] R. Toussaint *et al.*, Phys. Rev. E **69**, 011407 (2004).
[39] F. Jaber, Masters thesis, University of Bergen, 2003.